Numerical Analysis on the Current Distribution and the Loss in HTS Stacked Tapes Considering Termination Resistances

Ze Feng, Chengtao Wang, Rui Kang, and Qingjin Xu

***Abstract*—The high temperature superconducting (HTS) cables have wide application in superconducting magnets due to their high current-carrying capacity and thermal stability at high fields. But the current-carrying performance of the HTS cables is strongly affected by the current distribution among different tapes, which is usually determined by the resistance of the copper terminal. To investigate the mechanics of current distribution in the 15-strand stacked HTS tapes and further improve its performance, a simulation method considering both the splice resistance and the screening current effect has been set up by using the coupling of T-A formulation together with a circuit model. The numerical model could also be used to predict the critical performance of the cable and the losses in various conditions. The numerical model and the detailed result analysis are represented in this paper.**

***Index Terms*—Circuit, current distribution, critical current, losses, T-A formulation.**

I. Introduction

THE HTS cables made of second-generation coated conductors have a wide range prospects in the accelerator, nuclear fusion and power transmission due to their high current-carrying capacity and mechanical stability at high fields or high temperatures [2], [3], [4], [5], [6]. For such multi-strands, high-current superconducting cables, the critical performance and thermal stability of the HTS cable are strongly affected by the current distribution among the strands of the cable [1], [7]. Once there is a very large uneven current distribution among tapes, the cable would show a poor performance than expected or even end up with quench.

There are several factors that cause an uneven current distribution inside a superconducting cable. The n-value and the critical current (I_c) of commercial ReBCO tapes could vary along the length up to 10% [8]. These two parameters that depend on the angle and magnitude of the magnetic field can undergo a large variation. In addition, for non-transposed or partially transposed HTS cables, the difference of the inductance between the tapes would also cause a non-uniform current distribution [9]. Another important source of uneven current distribution is the terminal resistance. The variation of the joint resistance comes from different aging of the solder material and the manufacturing process [10].

The T-A formulation is an effective and accurate method to simulate the current distribution in a cable and coil made of HTS coated conductors [11], [12], [13], but it is inconvenient to be applied directly to the above cases. Here an alternative and more direct method is to couple the circuit into T-A formulation to solve this problem. The circuit module is used to calculate the current sharing between the superconducting tapes, and T-A formulation is employed to calculate the non-uniform current density distribution within HTS tapes.

In this article, we first introduce the T-A formulation and how it is coupled to the circuit. This model then is used to simulate the current distribution of a 4-tape cable. The predicted current distribution is consistent with the experimental data. Based on this method, we study the current distribution of the HTS cable consider the uniformity and magnitude of terminal resistance. Finally, the predicted critical currents and the losses of the HTS cable under different conditions are given.

II. Methodology and Validation

A. T-A Formulation

The *T* and the *A* are two state variables used in solving partial differential equations, where the *T* is the current vector potential and the *A* is the magnetic vector potential [14]:

$$B = \nabla \times A \tag{1}$$

$$J = \nabla \times T \tag{2}$$

where B and J are the magnetic flux density and the current density. Substituting (1) and (2) into Ampere's law and Faraday's law, we get:

$$\nabla \times \nabla \times A = \mu J \tag{3}$$

$$\nabla \times \rho_{HTS} \nabla \times T = -\frac{\partial B}{\partial t} \tag{4}$$

Manuscript received 25 September 2023; revised 7 December 2023, 29 December 2023, and 24 January 2024; accepted 29 January 2024. Date of publication 2 February 2024; date of current version 26 February 2024. This work was supported in part by the Chinese Academy of Sciences through Strategic Priority Research Program under Grant XDB25000000, in part by the Young Scientists Fund of National Natural Science Foundation of China under Grant 12005240, in part by Jialin Xie Fund under Grant E2546KU2, and in part by the National Key R&D Program of China under Grant 2018YFA0704203. *(Corresponding authors: Rui Kang; Qingjin Xu.)*

The authors are with the Laboratory of Particle Acceleration Physics and Technology, Institute of High Energy Physics, Chinese Academy of Sciences, Beijing 100049, China, and also with the University of Chinese Academy of Sciences, Beijing 100049, China (e-mail: fengze@ihep.ac.cn; kangrui@ihep.ac.cn; xuqj@ihep.ac.cn).

Color versions of one or more figures in this article are available at https://doi.org/10.1109/TASC.2024.3361441.

Digital Object Identifier 10.1109/TASC.2024.3361441

1051-8223 © 2024 IEEE. Personal use is permitted, but republication/redistribution requires IEEE permission.
See https://www.ieee.org/publications/rights/index.html for more information.

Authorized licensed use limited to: University of Durham. Downloaded on April 21,2026 at 15:54:09 UTC from IEEE Xplore. Restrictions apply.

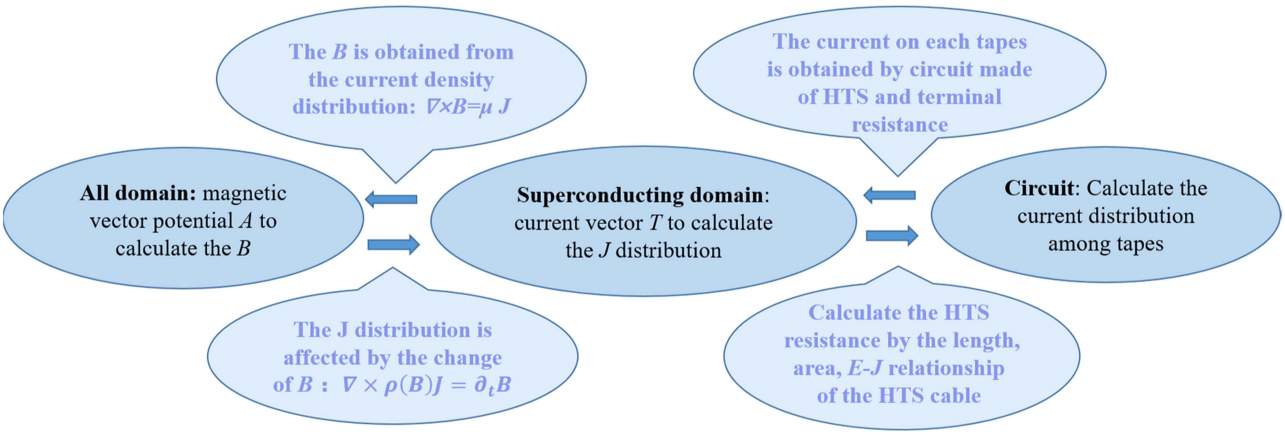

Fig. 1. How to complete the coupling of the T-A formulation and the circuit through different variables.

where ρ_{HTS} is the HTS resistivity. In the 2D case, we assume that the superconducting tape is infinitely long in the z-direction. Besides, the thickness of the superconducting layer is neglected [15]. Therefor J and T have only one non-zero component in z and x-direction. Consequently, (3) and (4) are simplified as follows:

$$\nabla^2 A_z = -\mu_0 J_z \tag{5}$$

$$\frac{\partial}{\partial y}\left(\rho_{HTS}\frac{\partial T_x}{\partial y}\right) = \frac{-\partial B_x}{\partial t} \tag{6}$$

where μ_0 is the vacuum permeability, A_z is the z- component of the magnetic vector potential and B_x is the x-component of magnetic flux density.

B. The Circuit

To simulate the current distribution among the tapes, the circuit model is introduced. Fig. 1 shows how to realize coupling of the T-A formulation with the circuit. In the superconducting element, the resistivity will be obtained by using a power-law.

$$\rho_{HTS,m} = \frac{E_c}{J_{c,m}}\left|\frac{J_m}{J_{c,m}}\right|^{n-1} \tag{7}$$

where the critical electric field E_c is 1×10^{-4} V·m^{-1}, $J_{c,m}$ is critical current density of the m-th tape. J_m is the current density flowing in the m-th element of the array, n is the quality index of the transition. Here all tapes have the same n-value.

The HTS resistance obtained by the T-A formulation is transferred to the circuit module for calculating the current distribution among the tapes. Then the distributed current of each tape is implemented in the boundary condition of the T-A formulation for simulating screening current. Fig. 2 is a schematic of the equivalent circuit model. The various materials (such as the copper stabilizer and the substrate) comprising the ReBCO tapes can be easily incorporated into the circuit model as the resistance element. Because the contact resistivity of our cable is 10^{-5}–10^{-6} Ω·m^2 by measurement for this cable. Its contact resistance is much higher than the HTS resistance. Therefore, the contact resistance is neglected. In our simulation the length of the cable is set as 1 m.

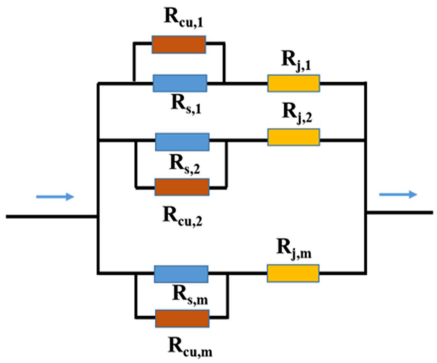

Fig. 2. Equivalent circuit diagram of HTS cables. $R_{s,m}$ is the superconducting resistance of the m-th tape , $R_{cu,m}$ is the copper layer of the superconducting tape of the m-th tape. $R_{j.m}$ is resistance of the joint between terminals and the m-th tape.

The current I_i flowing each tape solved by the circuit module is then applied to the corresponding tapes by the Dirichlet boundary condition.

$$\iint_\Omega J\, d\Omega = \iint_\Omega \nabla\times T\, d\Omega = \oint_{\partial\Omega} T\, dr = I_i \tag{8}$$

$$I_T = \sum_{i=1}^{m} I_i \tag{9}$$

where I_T is the total current, I_i is current of the i-th tape.

C. The Model Validation

To validate this numerical model, the current distribution in a simple stacked-tape cable is calculated. This cable consists of four tapes. There is a distance of 100 μm between them. In this case, these tapes in the cable have different joint resistances and critical currents. The geometry and performance parameters are listed in [1].

Fig. 3 presents the results of our numerical model, which are consistent with the experiment results in [1], [10]. In the low current, the current in each tape linearly rises, as the current distribution is mainly dominated by the termination resistance. the current sharing behavior changes in the high current. When

Authorized licensed use limited to: University of Durham. Downloaded on April 21,2026 at 15:54:09 UTC from IEEE Xplore. Restrictions apply.

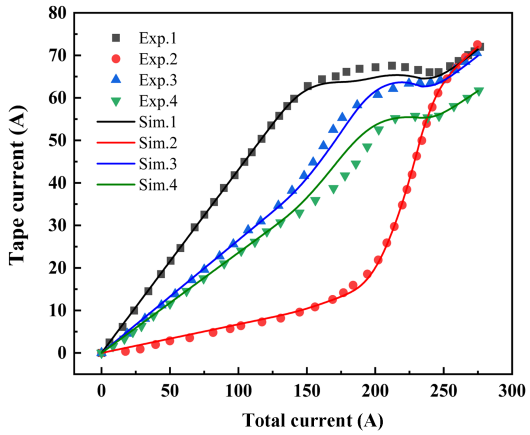

Fig. 3. Current of each tape versus total cable current. Solid line and dot respectively denote simulation and experiment results. Experimental results are from [1].

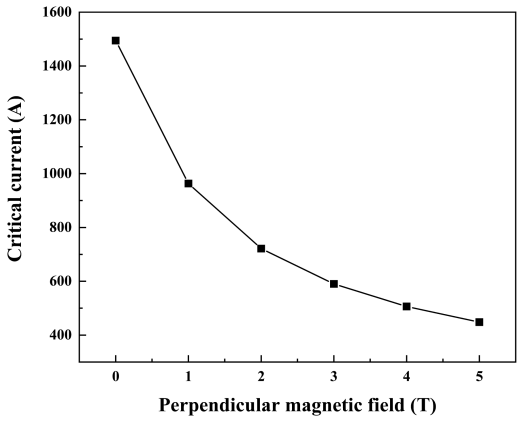

Fig. 4. Critical current of the superconducting tape in the cable as a function of the perpendicular magnetic field.

the individual current is close to the critical value, the resistance of HTS becomes non-negligible. Hence When the tape 1 reaches its critical current, the extra current begins to distribute over other tapes by the termination. The proposed numerical model can accurately simulate the current distribution in the HTS cable and also has been applied to our HTS cable.

III. Result and Discussion

Our cable is made of 15 75-μm thickness tapes stacked. The magnetic field dependence of the critical current is given by the interpolation function, which was fitted with the measured data given by the HTS tape manufacturer. Fig. 4 presents the perpendicular magnetic field dependence of the critical current at 4.2 K. The n value of tapes in the cable is 25. In addition, the charging speed is 20 A·s^{-1}. The T-A formulation and circuit module are applied in the 2D cross section of the HTS cable to predict the critical currents and the losses at the different conditions.

A. Non-uniform Terminal Resistance

In the joint manufacturing process, the uniformity and magnitude of the terminal resistance depend on the solder joint quality,

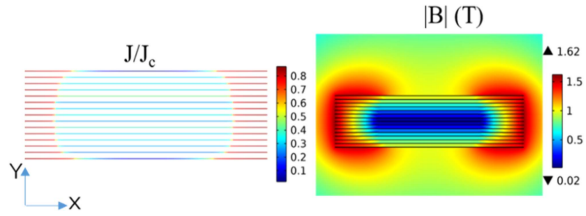

Fig. 5. Left figure is current density distribution at the total current 10000 A. Right figure is magnetic field distribution at the total current 10000 A.

TABLE I
Instantaneous Loss At Different Cable Current

	The cable current 5000A		The cable current 10000A	
R_j (nΩ)	The hysteresis loss in HTS (mW·m^{-1})	The loss of joint(mW)	The hysteresis loss in HTS (mW·m^{-1})	The loss of joint (mW)
10±0.5	0.212	17	8.9	68.2
10±2	0.222	16.5	9.39	66.2
10±5	0.302	14.3	16.4	58.2
100±5	0.211	169	8.95	674
100±20	0.234	154	9.81	614
100±50	0.293	174	79.1	707
400±2	0.212	653	8.99	2610
400±80	0.222	662	9.52	2650
400±20	0.375	504	253	2070

aging, and resistance of the Cu lead [7]. In this simulation, we assume that the joint resistance has three statistical distributions with low, middle and high standard deviations. Their average value is $<R_j> = 10$ nΩ; $<R_j> = 100$ nΩ; and $<R_j> = 500$ nΩ. The degree of deviation is $<\sigma> = 5\%$; $<\sigma> = 20\%$; $<\sigma> = 50\%$.

Fig. 5 shows current density distribution and magnetic field distribution at the total current 10000 A. Table I shows instantaneous loss at different cable currents, which is defined by $\int_\varphi E \cdot J \, d\varphi$, where φ is the superconductor domain. It is the hysteresis loss in HTS layer. Fig. 6 respectively show the current of each tape as a function of the total current at different terminal resistance. Fig. 7 shows the voltage in each tape as a function of the cable current at different terminal resistance.one Comparing Fig. 6(a3) to (c3), it shows that the higher deviation leads to a more unbalanced current distribution, which further leads to the attenuation of the critical current. Based on the 1 μV/cm criterion, the simulated critical currents at the $<R_j> = 400$ nΩ $<\sigma> = 5\%$ and the $<R_j> = 400$ nΩ $<\sigma> = 50\%$ are 14300 A and 8820 A, respectively. In addition, the loss for the high deviation 50% are 28 times at 10000 A of that for the low deviation 5% according to Table I. So the higher deviation leads to the smaller critical current and the higher loss.

Comparing Fig. 6(c1) to (c3), when the degree of the deviations is same, it shows that the bigger terminal resistance also leads to attenuation of the critical current. The simulated critical currents at the $<R_j> = 10$ nΩ $<\sigma> = 50\%$ and the $<R_j> = 400$ nΩ $<\sigma> = 50\%$ are 14992 A and 8820 A, respectively. In addition, the loss for the terminal resistance 400 nΩ are 15 times at 10000 A of that for the terminal resistance 10 nΩ. The main reason is the variation of the HTS resistance obtained by the E-J power law. For smaller terminal resistance, the HTS resistance influences on the current distribution at the high applied current.

Authorized licensed use limited to: University of Durham. Downloaded on April 21,2026 at 15:54:09 UTC from IEEE Xplore. Restrictions apply.

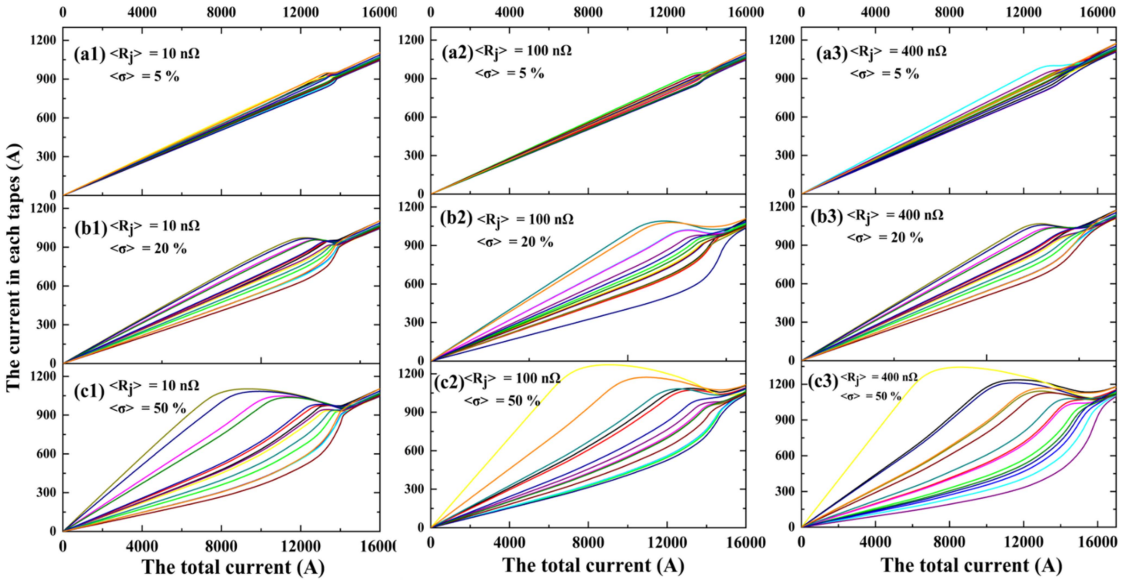

Fig. 6. Individual tape current as a function of the total current considering Gaussian distributed random values of terminal resistance. The average value of the terminal resistance is $<R_j> = 10\ n\Omega$; $<R_j> = 100\ n\Omega$; and $<R_j> = 500\ n\Omega$, They have three degree of deviations : $<\sigma> = 5\%$; $<\sigma> = 20\%$; $<\sigma> = 50\%$.

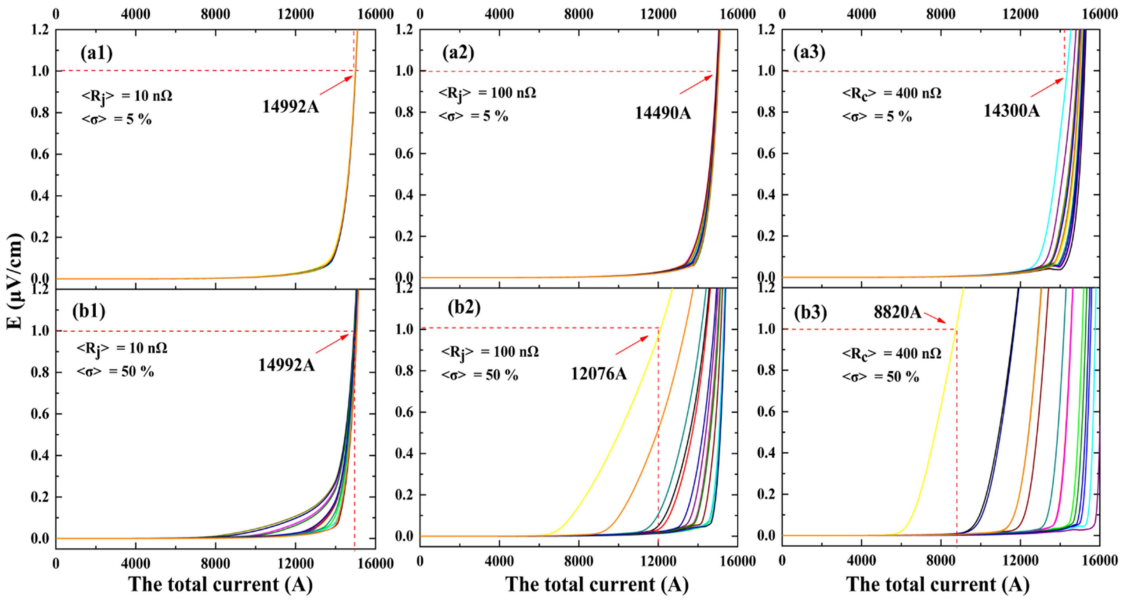

Fig. 7. Individual tape voltage as a function of the total current for different terminal resistance.

For larger terminal resistance, the HTS resistance has little influences on the current distribution. Even if a HTS tape in the cable gets more current to reach a critical state, it will still get more current because its resistance is much smaller than the terminal resistance.

IV. Conclusion

This paper introduces a numerical model based on the coupling of the T-A formulation and the circuit module. The circuit module calculates uneven current distribution caused by the difference of the terminal resistance, and the T-A formulation focuses on the screening current caused by the high aspect ratio of the ReBCO tapes. A four-tapes cable considering the joint resistance was used to verify the numerical model. The simulated current distribution has a good agreement with the experimental data. Hence this numerical method is applied to the 15-strand HTS cable to predict its critical currents and losses at different terminal resistances. The results show that a non-uniform terminal resistance can make the current distribution among tapes in the cable uneven. Such a large unbalance current distribution results in a large critical current decay and a large loss increase. In addition, a larger terminal resistance also results in a large critical current decay and a large loss increase. In contrast to terminal resistance($<R_j> = 10\ n\Omega$, $<\sigma> = 5\%$), the HTS cable considering terminal resistance ($<Rc> = 400\ n\Omega$, $<\sigma> = 50\%$) have a critical current degradation of 59% and a 28 times loss increase.

Authorized licensed use limited to: University of Durham. Downloaded on April 21,2026 at 15:54:09 UTC from IEEE Xplore. Restrictions apply.

REFERENCES

[1] V. Zermeno, P. Krüger, M. Takayasu, and F. Grilli, "Modeling and simulation of termination resistances in superconducting cables," *Supercond. Sci. Technol.*, vol. 27, no. 12, 2014, Art. no. 124013, doi: 10.1088/0953-2048/27/12/124013.

[2] G. A. Kirby et al., "Accelerator-quality HTS dipole magnet demonstrator designs for the EuCARD-2 5-T 40-mm clear aperture magnet," *IEEE Trans. Appl. Supercond.*, vol. 25, no. 3, Jun. 2015, Art. no. 4000805, doi: 10.1109/tasc.2014.2361933.

[3] J. S. Murtomaki, J. van Nugteren, G. Kirby, L. Rossi, J. Ruuskanen, and A. Stenvall, "Mechanical effects of the nonuniform current distribution on HTS coils for accelerators wound with REBCO Roebel cable," *IEEE Trans. Appl. Supercond.*, vol. 27, no. 4, Jun. 2017, Art. no. 4100405, doi: 10.1109/tasc.2017.2665882.

[4] J. M. Rey et al., "HTS Dipole insert developments," *IEEE Trans. Appl. Supercond.*, vol. 23, no. 3, 2013, Art. no. 4601004, doi: 10.1109/tasc.2013.2237931.

[5] B. N. Sorbom et al., "ARC: A compact, high-field, fusion nuclear science facility and demonstration power plant with demountable magnets," *Fusion Eng. Des.*, vol. 100, pp. 378–405, 2015, doi: 10.1016/j.fusengdes.2015.07.008.

[6] J. Zheng, Y. Song, X. Liu, K. Lu, and J. Qin, "Overview of the design status of the superconducting magnet system of the CFETR," *IEEE Trans. Appl. Supercond.*, vol. 28, no. 3, Apr. 2018, Art. no. 4204305, doi: 10.1109/tasc.2018.2797965.

[7] G. De Marzi, G. Celentano, A. Augieri, M. Marchetti, and A. Vannozzi, "Experimental and numerical studies on current distribution in stacks of HTS tapes for cable-in-conduit-conductors," *Supercond. Sci. Technol.*, vol. 34, no. 3, 2021, Art. no. 035016, doi: 10.1088/1361-6668/abda16.

[8] K. Jae-Ho, K. Chul Han, V. Pothavajhala, and S. V. Pamidi, "Current sharing and redistribution in superconducting DC cable," *IEEE Trans. Appl. Supercond.*, vol. 23, no. 3, 2013, Art. no. 4801304, doi: 10.1109/tasc.2013.2244153.

[9] D. Uglietti, R. Kang, R. Wesche, and F. Grilli, "Non-twisted stacks of coated conductors for magnets: Analysis of inductance and AC losses," *Cryogenics*, vol. 110, 2020, Art. no. 103118, doi: 10.1016/j.cryogenics.2020.103118.

[10] M. Takayasu, L. Chiesa, L. Bromberg, and J. V. Minervini, "HTS twisted stacked-tape cable conductor," *Supercond. Sci. Technol.*, vol. 25, no. 1, 2012, Art. no. 014011, doi: 10.1088/0953-2048/25/1/014011.

[11] V. M. R. Zermeno, F. Grilli, and F. Sirois, "A full 3D time-dependent electromagnetic model for Roebel cables," *Supercond. Sci. Technol.*, vol. 26, no. 5, 2013, Art. no. 052001, doi: 10.1088/0953-2048/26/5/052001.

[12] Y. Yan et al., "Screening-current-induced mechanical strains in REBCO insert coils," *Supercond. Sci. Technol.*, vol. 34, no. 8, 2021, Art. no. 085012, doi: 10.1088/1361-6668/ac0b2d.

[13] Y. Yan, T. Qu, and F. Grilli, "Numerical modeling of AC loss in HTS coated conductors and Roebel cable using T-A formulation and comparison with H formulation," *IEEE Access*, vol. 9, pp. 49649–49659, 2021, doi: 10.1109/access.2021.3067037.

[14] E. Berrospe-Juarez, F. Trillaud, V. M. R. Zermeno, F. Grilli, H. W. Weijers, and M. D. Bird, "Screening currents and hysteresis losses in the REBCO insert of the 32 T all-superconducting magnet using T-A homogenous model," *IEEE Trans. Appl. Supercond.*, vol. 30, no. 4, Jun. 2020, Art. no. 4600705, doi: 10.1109/tasc.2020.2969865.

[15] E. Berrospe-Juarez, F. Trillaud, V. M. R. Zermeño, and F. Grilli, "Advanced electromagnetic modeling of large-scale high-temperature superconductor systems based on H and T-A formulations," *Supercond. Sci. Technol.*, vol. 34, no. 4, 2021, Art. no. 044002, doi: 10.1088/1361-6668/abde87.

Authorized licensed use limited to: University of Durham. Downloaded on April 21,2026 at 15:54:09 UTC from IEEE Xplore. Restrictions apply.